FEBS Letters 582 (2008) 2869–2874

The three-dimensional structure of CsmA: A small antenna protein from the green sulfur bacterium *Chlorobium tepidum*

Marie Østergaard Pedersen[a], Jarl Underhaug[a], Jens Dittmer[a,*], Mette Miller[b], Niels Chr. Nielsen[a,*]

[a] *Center for Insoluble Protein Structures (inSPIN), Interdisciplinary Nanoscience Center (iNANO) and Department of Chemistry, University of Aarhus, Langelandsgade 140, DK-8000 Aarhus C, Denmark*
[b] *Department of Biochemistry and Molecular Biology, University of Southern Denmark, Campusvej 55, DK-5230 Odense M, Denmark*

Received 26 May 2008; revised 25 June 2008; accepted 12 July 2008

Available online 22 July 2008

Edited by Richard Cogdell

Abstract The structure of the chlorosome baseplate protein CsmA from *Chlorobium tepidum* in a 1:1 chloroform:methanol solution was determined using liquid-state NMR spectroscopy. The data reveal that the 59-residue protein is predominantly α-helical with a long helical domain extending from residues V6 to L36, containing a putative bacteriochlorophyll *a* binding domain, and a short helix in the C-terminal part extending from residues M41 to G49. These elements are compatible with a model of CsmA having the long N-terminal α-helical stretch immersed into the lipid monolayer confining the chlorosome and the short C-terminal helix protruding outwards, thus available for interaction with the Fenna–Matthews–Olson antenna protein.

Keywords: Chlorosome; CsmA; Green bacterium; Nuclear magnetic resonance; Photosynthetic antenna; *Chlorobium tepidum*

1. Introduction

The sun is the primary source of energy for living organisms. Despite great diversity in different light-dependent life forms, the basic principles of photosynthesis remain the same. A detailed understanding of the underlying processes is of great interest for basic research and for the potential realization of artificial photosynthetic devices with the perspective of energy conversion. The first element in a photosynthetic system is a light-harvesting antenna, which collects photons for further transmission of excitation energy to the reaction center [1]. The largest known antenna system is the chlorosome found in green sulfur bacteria. This antenna has an amazing capability to extract energy from low intensity light, exemplified by the findings of species able to survive 100 m below the surface of the Black Sea [2]. The chlorosome antenna system, which the green sulfur bacteria share with the green filamentous bacteria and the recently discovered aerobic phototroph Candidatus *Chloroacidobacterium thermophilum* [3], is unique in the sense that the main pigments, chlorosome chlorophylls, are self-organized in pigment–pigment complexes rather than pigment–protein complexes, as found in all other known photosynthetic antennae. This feature allows for a much higher pigment density and has served as inspiration for artificial antenna systems [4].

The green sulfur bacterium *Chlorobium* (*Chl.*) *tepidum* has chlorosomes containing multi-layered and single-layered tubular structures of self-aggregated bacteriochlorophyll (BChl) *c* [5]. The chlorosome is confined by a protein–lipid envelope [6], with 10 different proteins embedded in a monolayer of lipids [7]. Among these, the most abundant is the 59-residue chlorosome protein A (CsmA) [8] encoded for by the essential *csmA* gene [9]. CsmA binds BChl *a* and carotenoids [8,10,11] and comprise the so-called chlorosome baseplate, which can be observed as a 2D para-crystalline structure by freeze-fracture electron microscopy [12]. Following light-harvesting by BChl *c* aggregates, the excitation energy is transferred to the baseplate, then to the Fenna–Matthews–Olson (FMO) protein, a water-soluble antenna protein sandwiched between the chlorosome and the reaction centers in the plasma membrane (see schematic representation in Fig. 1).

The CsmA–BChl *a* baseplate complex is of particular interest as the simplest known antenna complex and may provide insight into the evolution of photosynthesis. We here present the first high-resolution structural model of CsmA isolated from chlorosomes derived from ^{15}N-labelled cells of *Chl. tepidum*, dissolved in deuterated chloroform:methanol, and analyzed using high-resolution ^{1}H NMR spectroscopy.

2. Materials and methods

2.1. Isolation of CsmA

Chl. tepidum ATCC 49652 was grown at 45 °C in the medium described by Wahlund et al. [13] with the modifications that NH_4–acetate was replaced by Na–acetate (0.5 g/L) and NH_4Cl was replaced by $^{15}NH_4Cl$ (0.4 g/L). Batch cultures were set up in 1 L bottles completely filled with medium in order to ensure anoxic conditions and illuminated with incandescent light giving a photon flux density of 14 μmol m^{-2} s^{-1}. After disrupting the cells by a French press, two consecutive sucrose density gradient centrifugations were applied to produce chlorosomes as described by Milks et al. [14]. Isolated chlorosomes were extracted with chloroform:methanol (1:1 by vol. containing 0.1 M ammonium acetate) and CsmA was purified from this extract as described previously [10].

2.2. NMR experiments

CsmA was dissolved in a small volume of trifluoroacetic acid, which was dried almost completely under a stream of nitrogen. The resulting protein film was dissolved in 400 μL CD_3OH:$CDCl_3$ (1:1 vol) to give a final concentration of 1.4 mM, as determined by

*Corresponding authors. Fax: +45 86 196199.
E-mail addresses: dittmer@chem.au.dk (J. Dittmer), ncn@inano.dk (N.Chr. Nielsen).

0014-5793/$34.00
doi:10.1016/j.febslet.2008.07.020

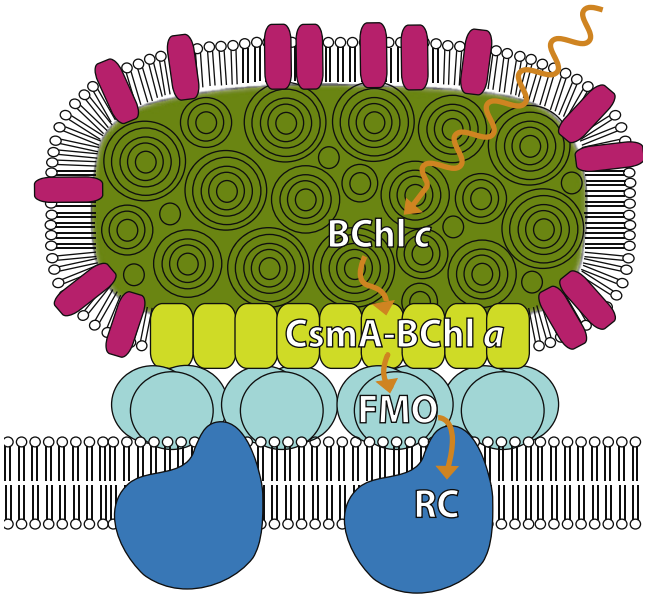

Fig. 1. Schematic representation of the photosynthetic system of *Chlorobium tepidum*. Orange arrows sum up the energy-transferring pathway: self-organized BChl *c* aggregates collect photons and the energy is sequentially transferred through two BChl *a* binding proteins: CsmA in the baseplate and the trimeric Fenna–Matthew–Olson (FMO) protein, ending in the special pair of the photosynthetic reaction centers (RC) situated in the cytoplasmic membrane. Envelope proteins apart from CsmA are shown in magenta.

the extinction coefficient (6970 M^{-1} cm^{-1} [10]). The solution was filled into a Shigemi NMR tube (Shigemi Co., Tokyo, Japan). All NMR spectra were recorded at 298 K.

^{1}H–^{1}H and ^{1}H–^{15}N NMR spectra were obtained on a Bruker Avance II 800 MHz spectrometer (18.8 T) equipped with a 5 mm triple-resonance TCI cryogenic probe: NOESY (τ_m = 200 ms) [15], TOCSY (τ_m = 25 and 80 ms) [16], COSY [17], HSQC [18], and 3D NOESY-HSQC spectra [19] were recorded. The signal of the non-deuterated alcohol group of methanol was suppressed using WATERGATE [20] and decoupling of ^{15}N during acquisition was achieved by the GARP sequence [21]. ^{15}N T_1 and T_2 measurements were carried out by sampling 6 or 7 time points within the intervals 0–1250 ms and 0–93 ms, respectively. A 3D HNHA spectrum [22] was recorded on a Bruker Avance II 700 MHz (16.4T) spectrometer using a standard 5 mm TXI triple-resonance probe, in order to obtain Karplus constraints on the torsion angle φ from $^{3}J_{HN,H\alpha}$ couplings. 2D ^{1}H–^{1}H spectra were recorded with 1000 increments in the indirect dimension (spectral width: 10 ppm) and 8 transients (NOESY: 16). The ^{1}H–^{15}N HSQC spectrum was acquired with 1000 increments and a spectral width of 22 ppm in the ^{15}N dimension and 4 transients, while the ^{15}N relaxation experiments used only 2 transients over 256 increments. The ^{1}H–^{15}N 3D NOESY-HSQC spectrum was acquired with 8 transients over 60 increments in the ^{15}N dimension (spectral width: 16 ppm) and 256 increments in the ^{1}H indirect dimension (spectral width: 10 ppm), while the HNHA spectrum acquired without cryogenic probe needed 32 transients over 60 increments in the ^{15}N dimension and 64 increments in the ^{1}H indirect dimension with the spectral widths as before. The spectra were processed using either Bruker Topspin or NMRPipe [23], and analyzed using SPARKY [24].

2.3. Structure calculation

Distance constraints from the NOESY and ^{1}H–^{15}N 3D NOESY-HSQC spectra and torsion angle constraints from the HNHA spectrum were used as input to a structure calculation by Ambiguous Restraints for Iterative Assignment (ARIA) 2.2 [25] in combination with the Crystallography and NMR System (CNS) [26]. A final set of 40 structures was generated, out of which the 14 structures with the lowest energy were subject to further analysis. Structures were analyzed using PROCHECK-NMR [27] and WHATIF [28] and visualized using PyMOL [29].

3. Results

2D and 3D spectra of ^{15}N-labelled CsmA in a 1:1 (vol) solution of chloroform:methanol were assigned manually. In addition to a dominant set of peaks straightforwardly assigned to the ^{1}H and ^{15}N atoms of CsmA, additional weak peaks were observed, as seen in the HSQC spectrum (Fig. 2), possibly stemming from a minor population of CsmA.

The atomic resolution structural model of CsmA was derived using 1426 structural NOE restraints, of which 805 were merged from peaks containing the same information. One thousand three hundred and fifty seven unambiguous peaks were assigned manually, whereas the rest was assigned by the algorithms implemented in ARIA (cf. Table 1). Karplus restraints from 31 *J* couplings were furthermore used as input for the structure calculation (Fig. 3, top). This structural model of CsmA is presented in Fig. 4a as an ensemble of the 14 lowest energy structures found after 9 iterations, and the average structure is seen in Fig. 4b. Overall, CsmA is an α-helical protein, as revealed from the structural ensemble, containing one long α-helix stretching over residues V6–L36 with a small bend around residues T28–M31. Furthermore, a short helix stretching over residues M41–G49 is present in the C-terminal part of the protein. The α-helical secondary structure is supported by many (*i*,*i* + 3) and (*i*,*i* + 4) NOE connectivities and *J* couplings below 6 Hz (Fig. 3, top). Enhanced backbone amide ^{15}N longitudinal (R_1) relaxation rates and in particular the low ^{15}N transverse (R_2) relaxation rates show a high flexibility on the ps time scale in both termini (Fig. 3, middle) – from residues M1 to G5 and from A47 to S59. This explains the high root mean square deviation (RMSD) values, for these parts of the protein (Fig. 3, bottom). Whereas the C-terminus contains only five flexible residues, which can be considered as normal for a protein in solution, the fast time scale flexibility at the N-terminus is increasing over a relatively wide range of 13 residues.

Consistently seen in all structure calculations are the bend of the long α-helix (T28–M31) and the break between the two α-helices (L36–M41), even though they are not clearly evident from the NOE connectivities or the relaxation data. From T28 to M31, the α-helix is unbroken explaining the high number of (*i*,*i* + 3) and (*i*,*i* + 4) NOE connectivities and the unchanged relaxation. On the other hand, the stretch from L36 to M41 shows a more turn-like structure with a break in the α-helix. Less (*i*,*i* + 3) and (*i*,*i* + 4) NOE connectivities are observed in this region than in the confined helices, and all of them are compatible with the break in the helix. We cannot observe a significant change of dynamics associated with this turn. No long-range constraints were established during assignment; there are no correlation peaks between amino acids spanning more than five amino acids, as it is expressed in the lack of any tertiary structure seen in the structural model.

4. Discussion

The solution NMR structure of CsmA purified from *Chl. tepidum* has been solved and is presented in Fig. 4. Under the present conditions (solution in 1:1 methanol:chloroform), CsmA is mainly an α-helical protein as evidenced clearly from

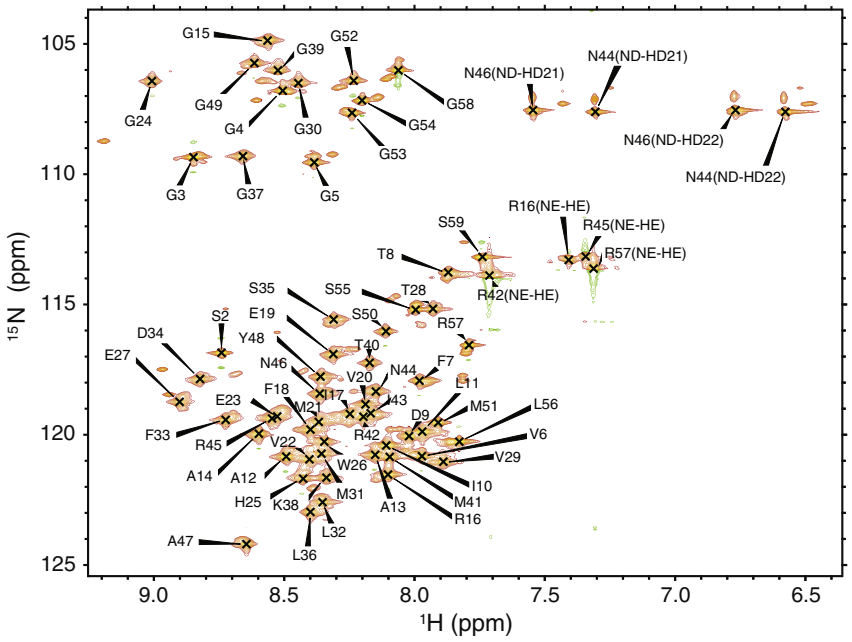

Fig. 2. HSQC spectrum of CsmA. Assignments of ^{1}H–^{15}N peaks (orange) are presented along with side chains containing nitrogen. Unassigned smaller peaks are ascribed to a minor conformation of the protein. Green color marks negative contour lines.

Table 1
Experimental restraints and structural statistics for CsmA

Experimental restraints	
Total restraints	1457
Merged	805
NOEs from ^{1}H–^{1}H NOESY	1186
Unambiguous	1117
NOEs from ^{1}H–^{15}N 3D NOESY-HSQC	240
Unambiguous	240
Distribution of NOEs	
Intraresidual	490
Sequential	338
Short range ($2 \leqslant i \leqslant 3$)	369
Medium range ($4 \leqslant i \leqslant 5$)	157
Long range ($i > 5$)	0
J couplings	31
Distance violations	
Mean number of NOE violations 0.2–0.5 Å	2.57 ± 0.851
Mean number of NOE violations > 0.5 Å	1.5 ± 0.855
Mean number of dihedral violations > 5°	0
RMSD values	
All atoms	6.300
Backbone atoms	5.903
All atoms aligned from residues 6 to 28	1.186
Backbone atoms aligned from residues 6 to 28	0.356
PROCHECK analysis (excl Gly-/end-residues)	
Favored regions	83.9 ± 3.2%
Additionally allowed regions	11.5 ± 3.0%
Generously allowed regions	4.5 ± 2.5%
Disallowed regions	0%

the pattern of distance and torsion constraints, and it holds no major tertiary structural fold.

The estimated helical content of CsmA in our structure is 66%. This value is higher than predicted from the amino acid sequence of CsmA. Theoretical helix propensity analysis suggested that the 59 residue CsmA protein has an α-helical content of 34% with one helix extending from residues 10 to 34, disrupted by the conserved GHW domain (residues 24–26) [30]. Similar findings were obtained using other secondary structure predicting programs. As opposed to the prediction

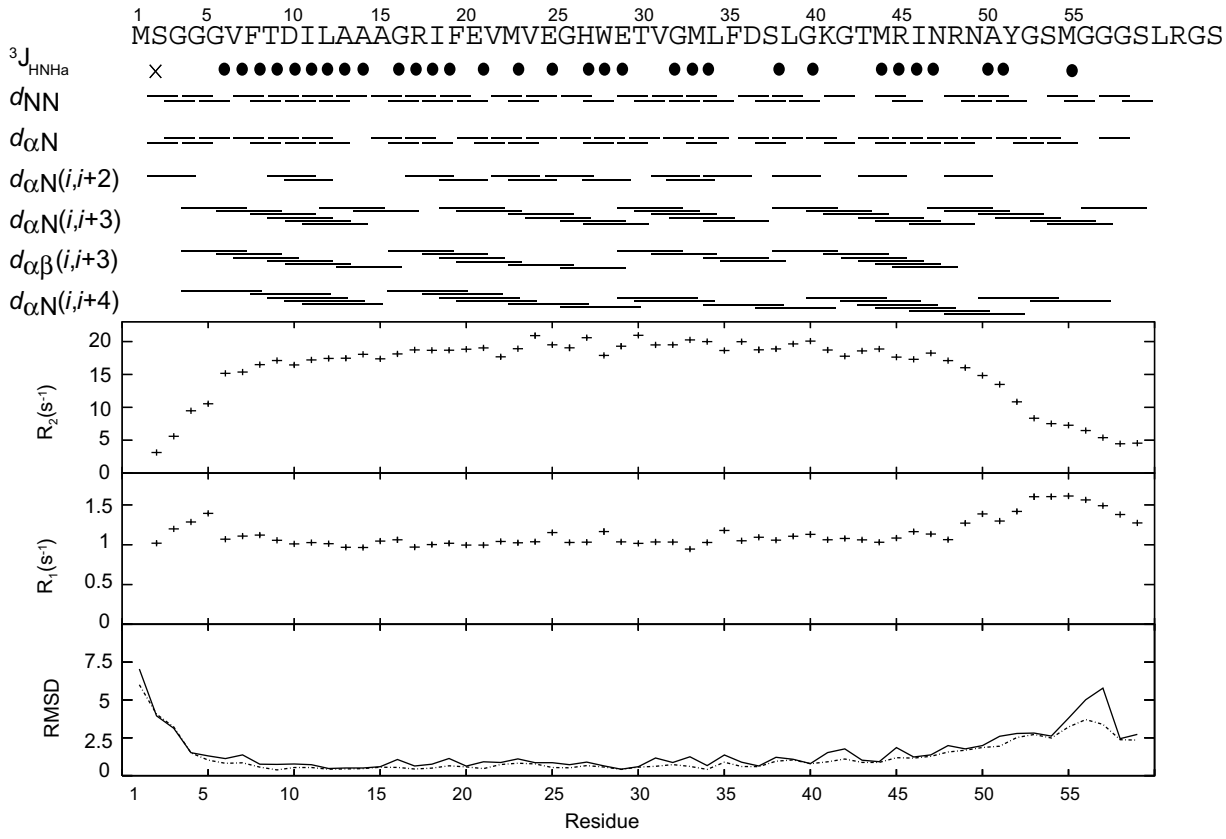

Fig. 3. NMR constraints and structure variability. Top-down: *J* couplings; filled circles indicate $^3J_{HNH\alpha} < 6$ Hz and cross indicates $^3J_{HNH\alpha} > 6$ Hz, NOE connectivities, backbone amide ^{15}N transverse relaxation rates (R_2), longitudinal relaxation rates (R_1), RMSD values including all atoms (solid line) and backbone atoms (dot-dashed line) with each alignment including five residues.

program, our results show that the helix is continued through the GHW domain, and an additional smaller helix is present in the C-terminal (M41–G49). By circular dichroism, we previously estimated an α-helix content of around 40% for isolated CsmA in detergent micelles of *n*-octyl β-D-glucopyranoside, whereas the α-helical content approximates 70% in a solution of trifluoroethanol [10], known to be an α-helix inducing solvent. The α-helical content of CsmA seems close to the α-helical content of the protein in trifluoroethanol (66% vs. ~70%) and significantly larger than of the protein in micelles (~40%) that match well with theoretical predictions (34%). These numbers suggest that the chloroform:methanol solvent also induce helicity of the CsmA protein. It has previously been observed that small, α-helical antenna proteins from purple bacteria retain their overall fold in chloroform:methanol [31,32], therefore we presume that the overall CsmA structure is representative, despite the noted discrepancies.

Previous studies of the topology of CsmA in isolated chlorosomes have suggested that the hydrophobic residues 2–39 are buried in the chlorosome envelope, while both the N-terminal M1 and the hydrophilic residues M41–S59 from the C-terminal are exposed [14]. In agreement with this, a high flexibility of the N-terminal (M1–G5) and C-terminal (A47–S59) was observed by the relaxation rates presented in Fig. 3. These findings suggest that the axis of the long α-helical stretch (V6–L36) is found parallel to the surface of the baseplate. The bend between the two helices around residues G37–T40 is most likely conserved in vivo allowing the short helix stretching from residues M41 to G49 and the remaining C-terminal to protrude out of the baseplate for interactions with the FMO protein [33]. It is interesting to note that the short helix contains the highly conserved sequence RINxNAY [33].

CsmA is known to form oligomers in the chlorosome baseplate [34] and dimer formation has been observed even under the denaturating conditions used for SDS–PAGE [35]. In addition, the protein has been observed to have limited solubility [10]. This propensity for aggregation might explain the minor CsmA population seen in the HSQC spectrum (Fig. 2). Near infra-red CD spectroscopy either on a baseplate preparation from *Chl. limicola* [36] or on a reconstituted complex between CsmA and BChl *a* in detergent micelles [10] have showed the characteristic spectrum of excitonic interactions between at least two BChl *a* molecules. In order to assemble two BChl *a* in close connection, we propose that in the intact baseplate of the *Chl. tepidum* chlorosomes, CsmA exists as dimers, which subsequently can be organized in long rows resulting in the 2D crystalline superstructure of the baseplate as observed by freeze-fracture electron microscopy [12].

As seen from the helical wheel presented in Fig. 5a, the envelope embedded and hydrophobic α-helix stretching over V6–T28 has an amphipathic nature. It is therefore tempting to position the hydrophilic part of this helix in the surface of the baseplate with dimerization occurring through hydrophobic interactions between two α-helices. H25, the candidate for BChl *a* coordination, is positioned exactly opposite of

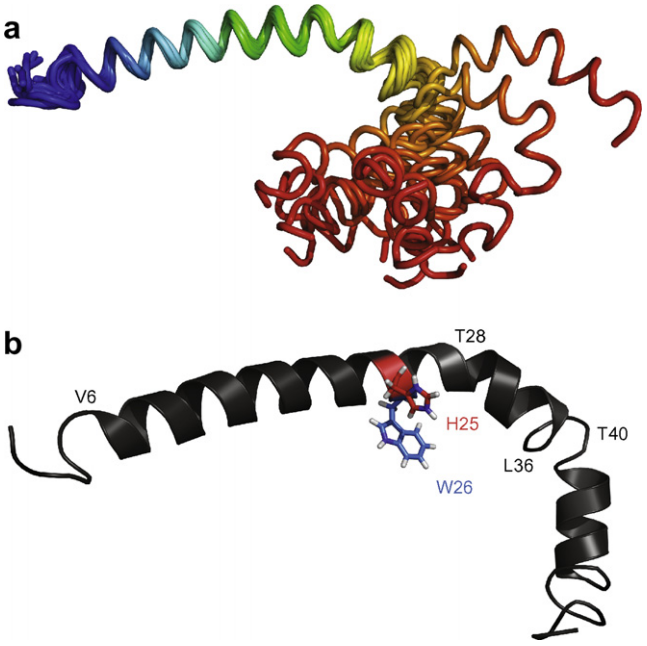

Fig. 4. NMR structure of CsmA. The structures are shown with the α-helical, chlorosome embedded part (residues S2–T40) at the top and the flexible N-terminal, which anchors CsmA to the FMO protein, pointing downwards. (a) The 14 lowest energy structures from an ensemble of 40. The structures are aligned from residues V6 to T28. (b) Average structure of CsmA. H25 and W26 are labeled in red and blue, respectively.

the hydrophilic residues and this arrangement will place H25 in the interior of the baseplate positioning the BChl *a* bacteriochlorin ring parallel with the surface of the baseplate. A drawback of this arrangement is that baseplate BChl *a* will be positioned far from the acceptor pigment in the FMO protein. Alternatively, dimerization might occur via electrostatic interactions involving the hydrophilic residues on opposing helices, as sketched in Fig. 5b and c. The helices might arrange in either a parallel or anti-parallel manner, and we arbitrarily chose the latter in our illustration in Fig. 5. In this hypothetical model, BChl *a* molecules are positioned by H25 in a hydrophobic environment between two CsmA dimers with the bacteriochlorin rings perpendicular to the baseplate surface, thus allowing for the observed excitonic interaction between two BChl *a* pigments described above being compatible with the chosen arrangement of the helices. We note, however, that more structural data is required to provide constraints for a more detailed dimerization model with a less arbitrary helix arrangement. Furthermore, in the model W26 can be positioned in the surface of the baseplate, as this amino acid has a preference for locating in water–lipid interfaces close to lipid head groups [37]. It is interesting to note that fluorescence anisotropy measurements on isolated chlorosomes derived from *Chloroflexus aurantiacus* have shown that the Q_y optical transition dipole moment of BChl *a* in the baseplate is almost perpendicular to the long axis of the chlorosomes [38] and this arrangement is also the case for chlorosomes of *Chl. tepidum* (H. Tamiaki, personal communication).

At present we are not able to provide further information on the detailed organization of the CsmA–BChl *a* complex in *Chl. tepidum*. We are currently using solid-state NMR to obtain structural data for CsmA and its interactions with BChl *a*.

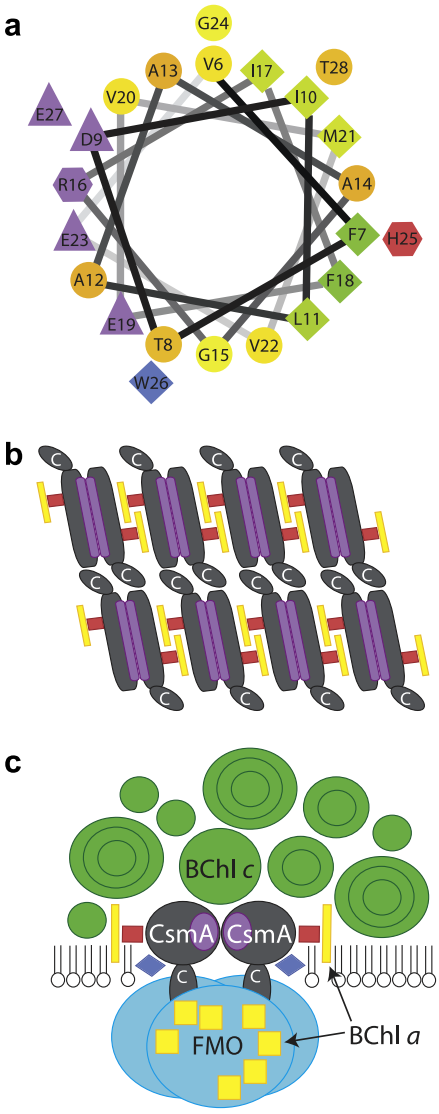

Fig. 5. Hypothetical model of the CsmA-BChl *a* arrangement in the chlorosome baseplate. (a) Helical wheel of V6-T28, compiled by [39]. (b) Top view of a hypothetical model of the arrangement of the amphipathic α-helix of CsmA (grey/purple) and BChl *a* (yellow) in the baseplate. The hydrophilic side of the helix is indicated by purple and the short C-terminal α-helix is labeled by the letter C. H25, believed to coordinate BChl *a*,is marked in red. (c) Side view of a hypothetical model of the CsmA–BChl *a* dimer. BChl *c* molecules are indicated as concentric circles (green) with the long axis of the chlorosome projecting into the page, and FMO is light blue with the 7 BChl *a* molecules marked in yellow. W26 (blue) is situated in the interface between lipid heads and tails in the chlorosome envelope.

Supplementary material

^{1}H and ^{15}N chemical shifts for CsmA have been deposited in the BioMagResBank (BMRB accession number 15742) and a structural ensemble is available at the RCSB Protein Data Bank (PDB ID code 2k37).

Acknowledgements: The research was funded by Danish National Research Foundation, The Danish Biotechnological Instrument Centre (DABIC), The Danish Natural Science Council, and Carlsbergfondet. We acknowledge the Danish Center for NMR of Biological Macromolecules at the Carlsberg Laboratory for the use of the Bruker Avance II 800 MHz spectrometer.

References

[1] Blankenship, R.E. (2002) Molecular Mechanisms of Photosynthesis, Blackwell Science, Malden, MA.

[2] Manske, A.K., Glaeser, J., Kuypers, M.A.M. and Overmann, J. (2005) Physiology and phylogeny of green sulfur bacteria forming a monospecific phototrophic assemblage at a depth of 100 meters in the Black Sea. Appl. Environ. Microb. 71, 8049–8060.

[3] Bryant, D.A., Costas, A.M.G., Maresca, J.A., Chew, A.G.M., Klatt, C.G., Bateson, M.M., Tallon, L.J., Hostetler, J., Nelson, W.C., Heidelberg, J.F. and Ward, D.M. (2007) Candidatus *Chloracidobacterium thermophilum*: an aerobic phototrophic acidobacterium. Science 317, 523–526.

[4] Balaban, T.S., Linke-Schaetzel, M., Bhise, A.D., Vanthuyne, N., Roussel, C., Anson, C.E., Buth, G., Eichhöfer, A., Foster, K., Garab, G., Gliemann, H., Goddard, R., Javorfi, T., Powell, A.K., Rösner, H. and Schimmel, T. (2005) Structural characterization of artificial self-assembling porphyrins that mimic the natural chlorosomal bacteriochlorophylls *c*, *d*, and *e*. Chemistry 11, 2267–2275.

[5] Oostergetel, G.T., Reus, M., Chew, A.G.M., Bryant, D.A., Boekema, E.J. and Holzwarth, A.R. (2007) Long-range organization of bacteriochlorophyll in chlorosomes of *Chlorobium tepidum* investigated by cryo-electron microscopy. FEBS Lett. 581, 5435–5439.

[6] Sørensen, P.G., Cox, R.P. and Miller, M. (2008) Chlorosome lipids from *Chlorobium tepidum*: characterization and quantification of polar lipids and wax esters. Photosynth. Res. 95, 191–196.

[7] Blankenship, R.E. and Matsuura, K. (2003) Antenna Complexes from Green Photosynthetic Bacteria. Light-harvesting Antennas in Photosynthesis, pp. 195–217, Kluwer Academic Publishers, Dordrecht, The Netherlands.

[8] Bryant, D.A., Vassilieva, E.V., Frigaard, N.U. and Li, H. (2002) Selective protein extraction from *Chlorobium tepidum* chlorosomes using detergents. Evidence that CsmA forms multimers and binds bacteriochlorophyll *a*. Biochemistry 41, 14403–14411.

[9] Chung, S.H., Shen, G.Z., Ormerod, J. and Bryant, D.A. (1998) Insertional inactivation studies of the *csmA* and *csmC* genes of the green sulfur bacterium *Chlorobium vibrioforme* 8327: the chlorosome protein CsmA is required for viability but CsmC is dispensable. FEMS Microbiol. Lett. 164, 353–361.

[10] Pedersen, M.Ø., Pham, L., Steensgaard, D.B. and Miller, M. (2008) A reconstituted light-harvesting complex from the green sulfur bacterium *Chlorobium tepidum* containing CsmA and bacteriochlorophyll *a*. Biochemistry. 47, 1435–1441.

[11] Montano, G.A., Wu, H.M., Lin, S., Brune, D.C. and Blankenship, R.E. (2003) Isolation and characterization of the B798 light-harvesting baseplate from the chlorosomes of *Chloroflexus aurantiacus*. Biochemistry 42, 10246–10251.

[12] Staehelin, L.A., Golecki, J.R. and Drews, G. (1980) Supramolecular organization of chlorosomes (chlorobium vesicles) and of their membrane attachment sites in *Chlorobium limicola*. Biochim. Biophys. Acta 589, 30–45.

[13] Wahlund, T.M., Woese, C.R., Castenholz, R.W. and Madigan, M.T. (1991) A thermophilic green sulfur bacterium from New Zealand hot-springs, *Chlorobium tepidum* Sp. Nov. Arch. Microbiol. 156, 81–90.

[14] Milks, K.J., Danielsen, M., Persson, S., Jensen, O.N., Cox, R.P. and Miller, M. (2005) Chlorosome proteins studied by MALDI-TOF-MS: topology of CsmA in *Chlorobium tepidum*. Photosynth. Res. 86, 113–121.

[15] Kumar, A., Ernst, R.R. and Wüthrich, K. (1980) A two-dimensional nuclear Overhauser enhancement (2D NOE) experiment for the elucidation of complete proton–proton cross-relaxation networks in biological macromolecules. Biochem. Biophy. Res. Co. 95, 1–6.

[16] Braunschweiler, L. and Ernst, R.R. (1983) Coherence transfer by isotropic mixing-application to proton correlation spectroscopy. J. Magn. Res. 53, 521–528.

[17] Aue, W.P., Bartholdi, E. and Ernst, R.R. (1975) Two-dimensional spectroscopy-application to nuclear magnetic resonance. J. Chem. Phys. 64, 2229–2246.

[18] Bodenhausen, G. and Ruben, D.J. (1980) Natural abundance ^{15}N NMR by enhanced heteronuclear spectroscopy. Chem. Phys. Lett. 69, 185–189.

[19] Marion, D., Kay, L.E., Sparks, S.W., Torchia, D.A. and Bax, A. (1989) Three-dimensional heteronuclear NMR of ^{15}N-labeled proteins. J. Am. Chem. Soc. 111, 1515–1517.

[20] Piotto, M., Saudek, V. and Sklenár, V. (1992) Gradient-tailored excitation for single-quantum NMR spectroscopy of aqueous solutions. J. Biomol. NMR 2, 661–665.

[21] Shaka, A.J., Barker, P.B. and Freeman, R. (1985) Computer-optimized decoupling scheme for wideband applications and low-level operation. J. Magn. Res. 64, 552–574.

[22] Vuister, G.W. and Bax, A. (1993) Quantitative *J* correlation – a new approach for measuring homonuclear three-bond *J* (H^N–H^α) coupling-constants in ^{15}N-enriched proteins. J. Am. Chem. Soc. 115, 7772–7777.

[23] Delaglio, F., Grzesiek, S., Vuister, G.W., Zhu, G., Pfeifer, J. and Bax, A. (1995) NMRpipe—a multidimensional spectral processing system based on unix pipes. J. Biomol. NMR 6, 277–293.

[24] Goddard, T.D. and Kneller, D.G. (1993) SPARKY-NMR Assignment and Integrating Software, University of California, San Francisco.

[25] Rieping, W., Habeck, M., Bardiaux, B., Bernard, A., Malliavin, T.E. and Nilges, M. (2007) ARIA2: automated NOE assignment and data integration in NMR structure calculation. Bioinformatics 23, 381–382.

[26] Brünger, A.T., Adams, P.D., Clore, G.M., DeLano, W.L., Gros, P., Grosse-Kunstleve, R.W., Jiang, J.S., Kuszewski, J., Nilges, M., Pannu, N.S., Read, R.J., Rice, L.M., Simonson, T. and Warren, G.L. (1998) Crystallography & NMR system: a new software suite for macromolecular structure determination. Acta Crystallogr. D 54, 905–921.

[27] Laskowski, R.A., MacArthur, M.W., Moss, D.S. and Thornton, J.M. (1993) PROCHECK: a program to check the stereochemical quality of protein structures. J. Appl. Crystallogr. 26, 283–291.

[28] Hooft, R.W.W., Vriend, G., Sander, C. and Abola, E.E. (1996) Errors in protein structures. Nature 381, 272.

[29] DeLano, W.L. (2002) The PyMOL Molecular Graphics System, DeLano Scientific, Palo Alto, CaliforniaCA.

[30] Raghava, G.P.S. (2000) Protein secondary structure prediction using next neighbor and neural network approach. CASP4, 74–76.

[31] Kikuchi, J., Asakura, T., Loach, P.A., Parkes-Loach, P.S., Shimada, K., Hunter, C.N., Conroy, M.J. and Williamson, M.P. (1999) A light-harvesting antenna protein retains its folded conformation in the absence of protein–lipid and protein–pigment interactions. Biopolymers 49, 361–372.

[32] Conroy, M.J., Westerhuis, W.H.J., Parkes-Loach, P.S., Loach, P.A., Hunter, C.N. and Williamson, M.P. (2000) The solution structure of *Rhodobacter sphaeroides* LH1 beta reveals two helical domains separated by a more flexible region: Structural consequences for the LH1 complex. J. Mol. Biol. 298, 83–94.

[33] Pedersen, M.Ø., Borch, J., Højrup, P., Cox, R.P. and Miller, M. (2006) The light-harvesting antenna of *Chlorobium tepidum*: interactions between the FMO protein and the major chlorosome protein CsmA studied by surface plasmon resonance. Photosynth. Res. 89, 63–69.

[34] Li, H., Frigaard, N.U. and Bryant, D. (2006) Molecular contacts for chlorosome proteins revealed by cross-linking studies with chlorosomes from *Chlorobium tepidum*. Biochemistry 45, 9095–9103.

[35] Frigaard, N.U., Li, H., Martinsson, P., Das, S.K., Frank, H.A., Aartsma, T.J. and Bryant, D.A. (2005) Isolation and characterization of carotenosomes from a bacteriochlorophyll *c*-less mutant of *Chlorobium tepidum*. Photosynth. Res. 86, 101–111.

[36] Gerola, P.D. and Olson, J.M. (1986) A new bacteriochlorophyll *a* –protein complex associated with chlorosomes of green sulfur bacteria. Biochim. Biophys. Acta 848, 69–76.

[37] Yau, W.M., Wimley, W.C., Gawrisch, K. and White, S.H. (1998) The preference of tryptophan for membrane interfaces. Biochemistry 37, 14713–14718.

[38] Shibata, Y., Saga, Y., Tamiaki, H. and Itoh, S. (2007) Polarized fluorescence of aggregated bacteriochlorophyll *c* and baseplate bacteriochlorophyll *a* in single chlorosomes isolated from *Chloroflexus aurantiacus*. Biochemistry 46, 7062–7068.

[39] Armstrong, D and Zidovetzki, R (2001) wheel.pl. <http://rzlab.ucr.edu/scripts/wheel/wheel.cgi>.